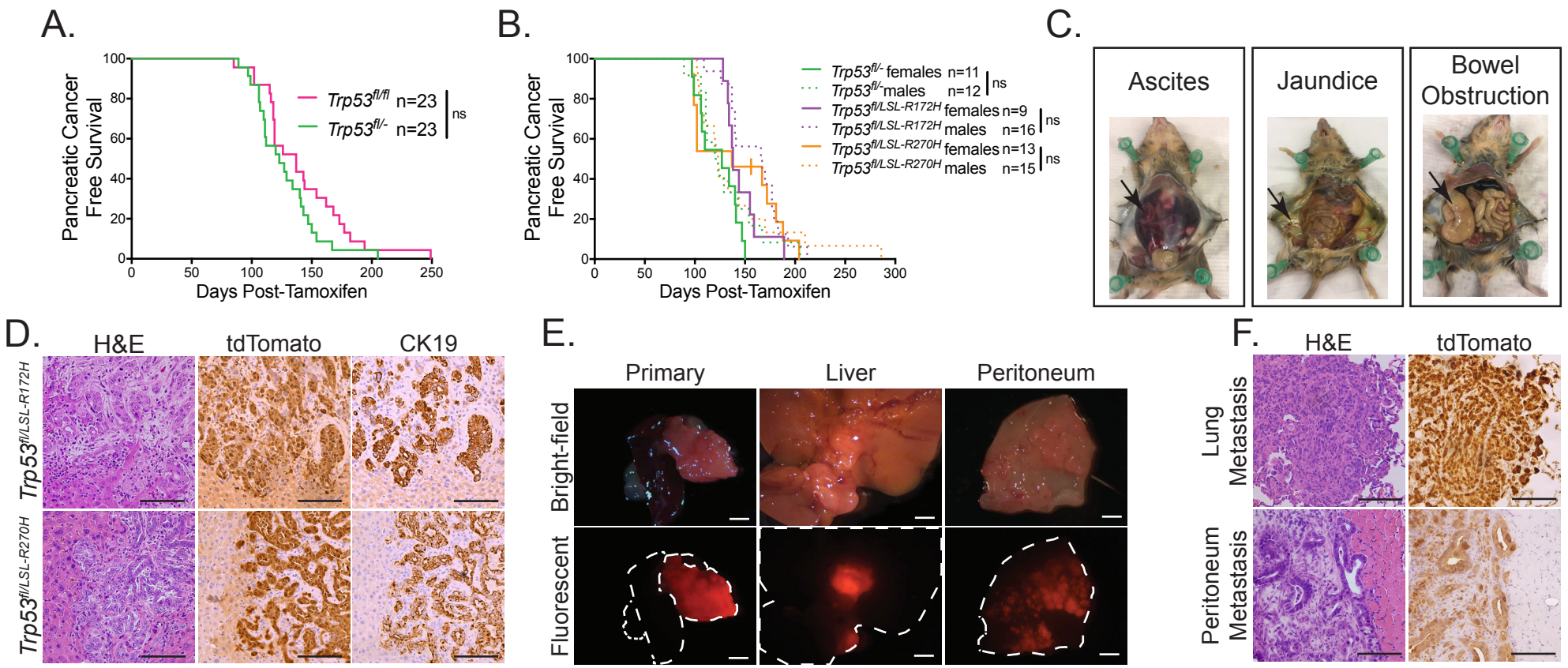

Supplementary Figure 2. Analysis of p53 missense mutants in acinar cell-derived pancreatic cancer development

(A) Kaplan-Meier analysis comparing pancreatic cancer-free survival of two different models of p53 deficiency. Pancreatic cancer incidence in *KT;Ptf1a^{CreER};Trp53$^{fl/fl}$* mice (n = 23) and *KT;Ptf1a^{CreER};Trp53$^{fl/-}$* mice (n = 23), based on the log-rank test. Not significant = ns. **(B)** Kaplan-Meier analysis of pancreatic cancer-free survival of *KT;Ptf1a^{CreER};Trp53$^{fl/x}$* (where x represents different *Trp53* alleles) cohorts listed in Figure 2A and stratified by sex. Pancreatic cancer incidence in *KT;Ptf1a^{CreER};Trp53$^{fl/-}$* female mice (n = 11) and male mice (n = 12) is similar based on the log-rank test. Pancreatic cancer incidence in *KT;Ptf1a^{CreER};Trp53$^{fl/LSL-R172H}$* female mice (n = 9) and male mice (n = 16) is similar based on the log-rank test. Pancreatic cancer incidence in *KT;Ptf1a^{CreER};Trp53$^{fl/LSL-R270H}$* female mice (n = 13) and male mice (n = 15) is similar based on the log-rank test. Not significant = ns. **(C)** Representative images of mice presenting with ascites, jaundice, or bowel obstruction in each cohort. **(D)** Representative histological image of a liver metastases in a *KT;Ptf1a^{CreER};Trp53$^{fl/LSL-R172H}$* and a *KT;Ptf1a^{CreER};Trp53$^{fl/LSL-R270H}$* mouse analyzed by H&E staining and immunohistochemistry for tdTomato and CK19. Scale Bar = 100 μm. **(E)** Representative bright-field and fluorescence dissecting scope images of a primary acinar cell-derived tumor and liver and peritoneum with macroscopic metastases. Scale Bar = 2 cm **(F)** Representative histological images of a lung metastasis in a *KT;Ptf1a^{CreER};Trp53$^{fl/LSL-R270H}$* mouse and a peritoneum metastasis in a *KT;Ptf1a^{CreER};Trp53$^{fl/-}$* mouse analyzed by H&E staining and tdTomato immunostaining. Scale Bar = 100 μm.